Journal of Asian Earth Sciences 137 (2017) 241–249

Contents lists available at ScienceDirect

Journal of Asian Earth Sciences

journal homepage: www.elsevier.com/locate/jseaes

Full length article

Newly discovered uranium mineralization at ~2.0 Ma in the Menggongjie granite-hosted uranium deposit, South China

Jin-Cheng Luo [a,b], Rui-Zhong Hu [a,*], Mostafa Fayek [b], Xian-Wu Bi [a], Shao-Hua Shi [c], You-Wei Chen [a]

[a] State Key Laboratory of Ore Deposit Geochemistry, Institute of Geochemistry, Chinese Academy of Sciences, Guiyang 550081, China
[b] Department of Geological Sciences, University of Manitoba, Winnipeg R3T 2N2, Canada
[c] Hunan Institute of Geological Survey, Changsha 410116, China

ARTICLE INFO

Article history:
Received 18 October 2016
Received in revised form 17 January 2017
Accepted 18 January 2017
Available online 21 January 2017

Keywords:
Menggongjie
SIMS U-Pb
Granite-hosted
Uranium deposit
South China

ABSTRACT

The southeastern part of the Nanling metallogenic province, South China contains numerous economically important granite-hosted, hydrothermal vein-type uranium deposits. The Miao'ershan (MES) uranium ore field is one of the most important uranium sources in China, hosts the largest Chanziping carbonaceous-siliceous-pelitic rock-type uranium deposit and several representative granite-hosted uranium deposits. The geology and geochemistry of these deposits have been extensively studied. However, accurate and precise ages for the uranium mineralization are scarce because uranium minerals in these deposits are usually fine-grained, and may have formed in several stages, thus hindering the understanding of the uranium metallogenesis of this province.

The Menggongjie (MGJ) uranium deposit is one of the largest granite-hosted uranium deposits in the MES ore field. Uranium mineralization in this deposit occurs at the central part of the MES granitic complex, accompanied with silicification, fluorination, K-metasomatism and hematitization. The ore minerals are dominated by uraninite, occurring in quartz or fluorite veinlets along fractures in altered granite. *In-situ* SIMS U-Pb dating on the uraninite yields the U–Pb isotopic age of 1.9 ± 0.7 Ma, which is comparable to the chemical U-Th-Pb^{tot} uraninite age of 2.3 ± 0.1 Ma. Such ages agree well with the eruption ages of the extension-related Quaternary volcanics (2.1–1.2 Ma) in South China, suggesting that the uranium mineralization have formed at an extensional setting, possibly related to the Quaternary volcanic activities. Therefore, our robust, new dating results of the MGJ uranium deposit make it the youngest granite-hosted uranium deposit reported so far in South China and the mineralization event represents a newly identified mineralization epoch.

1. Introduction

The Mesozoic South China is characterized by the widespread magmatism and economically important granite-related W–Sn–Cu–U–REE mineralization. The South China uranium metallogenic province accounts for the largest known source of uranium in China. Previous studies have revealed that the granite-hosted uranium ore deposits are important commercial uranium producers in South China (Fig. 1) (e.g., Hu et al., 2004, 2008; Chen et al., 2012; Luo et al., 2015a; Zhao et al., 2016), providing ca.30% of the uranium sources in China during the past three decades. Similar granite-hosted uranium deposits elsewhere in the world include those in the Hercynian granites of the La Crouzille district of the Massif Central, France (e.g., Cuney, 1978; Leroy, 1978; Turpin et al., 1990), the Eastern Desert of Egypt (e.g., El-Naby, 2009; Helmy et al., 2014), and the Moldanubian Zone of the Bohemian Massif (e.g., Kribek et al., 1999; Dolníček et al., 2014).

Numerous mineral exploration and scientific studies have shown that the uranium deposits are closely associated with their host granitic bodies (e.g., Hu and Jin, 1990; Hu et al., 1993, 2008; Min et al., 1999, 2005; Shi et al., 2010; Chen et al., 2012; Luo et al., 2015a,b; Zhao et al., 2016). Generally, these U-bearing granites are rich in uranium (>12 ppm) with leachable uranium sources such as the Guidong granitic complex (Chen et al., 2012; Luo et al., 2015a) and Douzhashan granite (Luo et al., 2015b; Zhao et al., 2016), which have been regarded as the main sources of uranium mineralization. These granites were emplaced in the Triassic or the Jurassic (e.g., Hu et al., 2004, 2008; Chen et al., 2012; Deng et al., 2012; Zhao et al., 2014), whereas the uranium deposits are considered to have formed from the circulation of meteoric fluids during the Cretaceous to Tertiary crustal extension in South China

* Corresponding author.
E-mail address: huruizhong@vip.gyig.ac.cn (R.-Z. Hu).

http://dx.doi.org/10.1016/j.jseaes.2017.01.021
1367-9120/

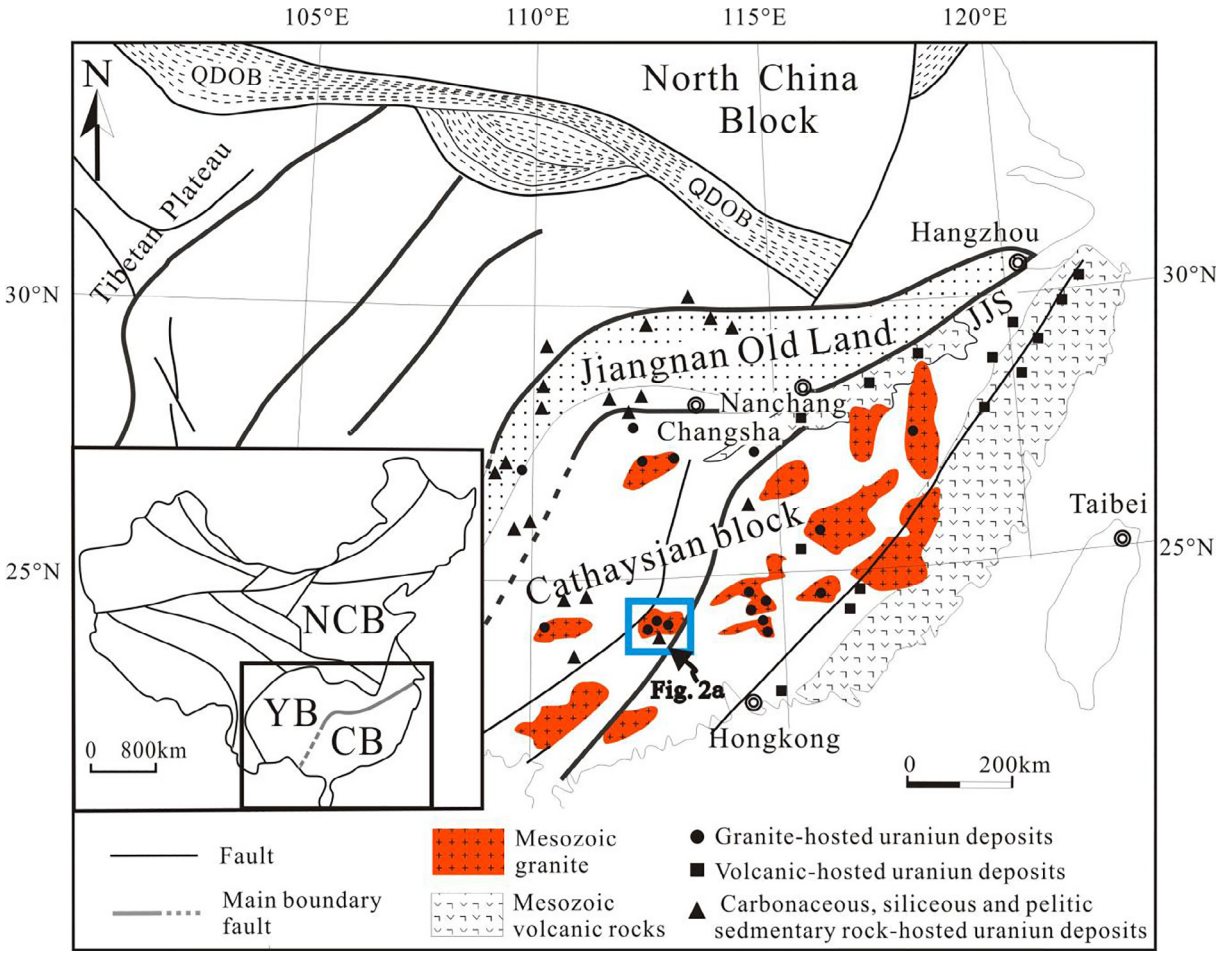

Fig. 1. Maps showing the tectonic units and distribution of uranium deposits in South China (Hu et al., 2008).

(Hu et al., 2008; Luo et al., 2015a). Recently, the timing and petrogenesis of these U-bearing granites in South China have attracted attention for past decades (e.g., Hu and Jin, 1988; Deng et al., 2012; Chen et al., 2012; Hu et al., 2012, 2013; Zhao et al., 2013, 2014). Although numerous studies have been carried out the ore-forming ages of uranium deposits in South China (e.g., Xu et al., 1988; Xu and Zhang, 1988; Fang et al., 2007; Hu et al., 2004, 2008; Shi et al., 2010; Tian et al., 2010; Chen et al., 2012; Hu et al., 2013), these mineralization ages are yet to be verified by direct dating of uranium minerals from these deposits. In addition, these studies relied on bulk analytical techniques, which were not able to discriminate between distinct generations of fine-grained uranium minerals and alteration zones that may occur at a micron-scale. Thus, the ages, geochemistry and sources of these uranium deposits in the southeastern part of the Nanling metallogenic province, are still poorly understood. To date, a number of geologic models have been proposed for granite-hosted uranium deposits, including leaching of uranium from the host granite by mixed oxidized meteoric and basin fluids (e.g., Turpin et al., 1990; Dolníček et al., 2014), hot spot uranium metallogenesis closely related to deep mantle plume tectonics (Li, 2006) and mantle-degassing associated with mafic magmatism in an extensional setting (e.g., Hu et al., 2008; Luo et al., 2015a). In particular, ore-forming ages for the associated fluid events and the genetic process of these granite-hosted uranium deposits in South China are still lacking.

The Miao'ershan (MES) granitic batholith has a total outcrop area of ca. 1633 k^2, including an important granite-hosted uranium ore district (Fig. 2).The Douzhashan granite, located in the middle of the MES granitic complex (Fig. 2a), is one of important U-bearing granites in South China, with extremely high uranium concentrations (up to 26 ppm) (Zhao et al., 2016). It hosts several hydrothermal vein-type uranium deposits, including the Menggongjie, Shazijiang, Baimaochong, and Shuanghuajiang deposits (Fig. 2). However, only few studies have been done on these deposits since their discovery in 1980s (Xu et al., 1988; Xu and Zhang, 1988; Fang et al., 2007; Shi et al., 2010; Huang et al., 2012). Until now, reliable ages for the uranium mineralization have not been reported, thus hindering our understanding of the origin of the uranium mineralization in the MGJ deposit. In this study, we described the main uranium mineralization in the MGJ uranium deposit, South China, and obtained *in-situ* SIMS U–Pb and chemical U-Th-Pb ages of uraninites. Our new results indicate that the uranium mineralization in the MGJ deposit represents a newly discovered Quaternary metallogenic event in South China.

2. Geological background

The South China Block in the southeastern part of the Eurasian continent is made up of the Yangtze and Cathaysia Blocks, which were welded together along the Jiangnan orogenic belt during the Neoproterozoic (Zhao et al., 2011). It is bounded by the North China Craton to the north, the Songpan-Ganzi Terrane of the Tibetan Plateau to the northwest, and the Indochina Craton to the south. South China underwent three major tectonic-magmatic

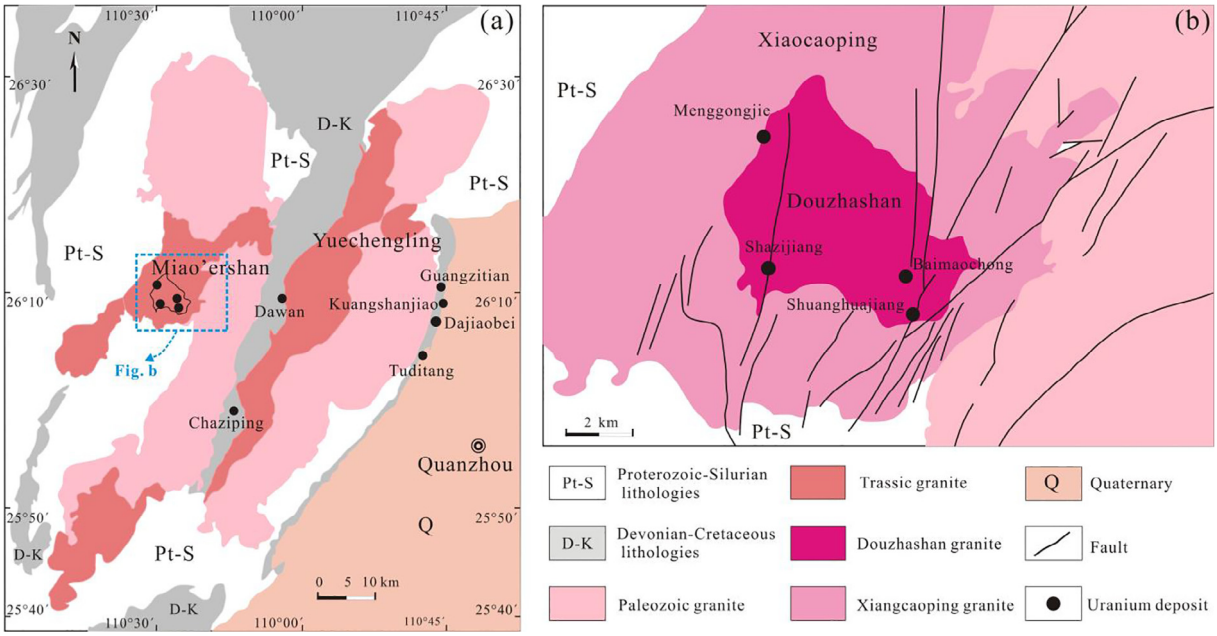

Fig. 2. The Miao'ershan-Yuechengling granitic batholith (a) and the uranium deposits in the Douzhashan and Xiangcaoping granites (b) (modified from Shi et al., 2010; Zhao et al., 2014).

events after its formation, and abundant igneous rocks, especially granitoids and granite-related metal deposits, formed in response to these events (e.g., Zhou et al., 2006; Li and Li, 2007; Hu and Zhou, 2012). It is also well known for its large-scale mineralization during the Mesozoic, making the region one of the most important polymetallic metallogenic provinces in the world. Hu and Zhou (2012) classified these deposits in South China into polymetallic hydrothermal systems closely related to felsic intrusive rocks (W-Sn-Mo granites, Cu porphyries, polymetallic and Fe skarns, and polymetallic vein deposits) and low-temperature hydrothermal systems with no direct connection to igneous activities (MVT deposits, epithermal Au and Sb deposits). These spectrums of deposits formed in the Triassic (Indosinian), Jurassic-Cretaceous (Early Yanshanian), and Cretaceous (Late Yanshanian).

South China is rich in granite-hosted vein-type uranium deposits, which have been a main source of uranium for China. The Miaoer'shan-Yuechengling (MES-YCL) granitic belt is one of the most important W-Sn-U-polymetallic metallogenic belts in the Nanling region. The core unit of the MES-YCL anticlinorium consists of Neoproterozoic-Silurian carbonaceous slates, pelitic schists, felsic volcaniclastics, metasandstones and dolostones. The Miao'ershan (MES) granitic rocks intruded into the core of the MES-YCL anticlinorium, forming a large batholith and extending from northern Guangxi province to southern Hunan province, and represent the most western part of the Nanling granite belt in South China. Recently, Zhao et al. (2013) have revealed that the MES granitic batholith is composed of Paleozoic granites and Triassic granites. The Triassic granites include the Xiangcaoping and Douzhashan granites in the center and the Yangqiaoling granite in the southern part of the batholith.

The MES area is one of the most important uranium ore fields in the Nanling uranium metallogenic province, and contains the largest Chanziping carbonaceous-siliceous-pelitic rock-type uranium deposit, and Menggongjie, Shazijiang, and shuanghuajiang granite-hosted uranium deposits (Fig. 2a). The Douzhashan granite occurred in the middle part of the MES granitic plutons. The ore bodies of the MGJ granite-hosted uranium deposit are distributed along the contact between the Xiangcaoping and Douzhashan granite, covering a mineralized area of only 32 km^2 (Fig. 2b). The Douzhashan granite pluton has higher uranium contents than coeval granites and has been regarded as the main source of uranium for the granite-hosted deposit in the MES ore field (Min et al., 2003; Hu et al., 2012; Luo et al., 2015b; Zhao et al., 2016). In addition to the MES granite-hosted uranium ore field, the Nanling uranium metallogenic province are also well known for its carbonaceous-siliceous-pelitic rock-type Quanzhou uranium ore district in the late Paleozoic basin, located in the edge of the YCL granitic batholith, such as the Guangzitian, Tuditang and Dajiaobei deposits. These uranium deposits generally occur within the Douzhashan pluton, contact zones and faults (Fig. 2b).

3. Deposit geology

Several middle- and large-scale uranium deposits (e.g. Menggongjie, Shazijiang, Shuanghuajiang and Baimaochong) have been found within the Douzhashan pluton (Fig. 2b). The orebodies in these deposits occur as veins controlled by NE- and NNE-trending faults which cut through the Douzhashan and Xiangcaoping granites, but uranium mineralization is spatially associated with the Douzhashan granite. The Douzhashan granite pluton is composed of medium- to coarse-grained two-mica granite with a zircon U-Pb age of 203 ± 4 Ma and muscovite ^{39}Ar-^{39}Ar age of 207 ± 4 Ma (Zhao et al., 2014). It is the youngest pluton in the MES complex, emplaced during the late Indosinian stage in a post-collisional setting (Zhao et al., 2014). In contrast, the other U-bearing granites in South China were emplaced during the early Indosinian with a syn-collisional setting (e.g., Xiazhuang and Zhuguang granitic composite, Chen et al., 2012; Deng et al., 2012). In addition to the intrusion ages of these granites in the MES ore field, Luo et al. (2015b) obtained an age of 70.2 ± 1.6 Ma for the major uranium mineralization in the Shazijiang granite-hosted uranium deposit, which is nearly identical to that of the Chanziping carbonaceous-siliceous-pelitic rock-type uranium deposit (75 ± 4 Ma; Xu et al., 1988). Such a mineralization stage is more widespread and refers to various different types of uranium depos-

its, probably indicating a large-scale uranium metallogenesis in South China during late Cretaceous (Luo et al., 2015b). Moreover, Hu et al. (2013) reported a chemical age of ~136 Ma for the secondary apatite from the Douzhashan granite, which was suggested to be coeval with the Cretaceous crustal extension in south China. In summary, previous studies have shown that the uranium mineralization in the MES ore distinct mainly occurred at ~136, 105 to 95, ~75 Ma (Xu et al., 1988; Xu and Zhang, 1988; Fang et al., 2007; Hu et al., 2008, 2013; Shi et al., 2010; Luo et al., 2015b), which are far younger than the emplacement age of the Douzhashan granite.

The MGJ deposit contains uranium ores with an average grade of ~0.2–0.7% U. The largest ore body is ~180 m in length and ~1.5 m in width. The ore bodies are structurally controlled and confined to shear zones and fault planes within the Douzhashan granitic pluton. The fault zones are filled with breccias cemented by coarse- to medium- grained quartz, calcite and fluorite, and have been mostly activated during late Indosinian (Early Jurassic) to late Yanshanian (Late Cretaceous) (Fang et al., 2007). The uranium mineralization is present as discontinuous veinlets and irregular patches, associated with deep violet fluorite, smoky quartz, hematitization and silicification of the host granites (Fig. 3a). The ore minerals in the deposit are dominated by uraninite and sooty pitchblende at depth with uranophane, autunite (Fig. 3b-d) and secondary uranyl minerals at higher levels (Fig. 3a). The deposit has a paragenetic sequence including an early uraninite-microcrystalline quartz stage, followed by uraninite-pyrite and late uraninite-hematite stages.

4. Analytical methods

4.1. Electron microprobe (EMP) analysis

The chemical composition of the MGJ uraninite was determined using a Cameca SX100 electron microprobe equipped with a PGT energy-dispersive spectrometer and five wavelength-dispersive spectrometers. EMP analyses were carried out at the Department of Geological Sciences, University of Manitoba. The analytical conditions were a 15 keV accelerating voltage, 20 nA beam current and a 5 μm beam diameter. Diopside, UO_2, titanite, fayalite, PbTe, andalusite, ThO_2, pyrite, albite, orthoclase, VP_2O_7 and apatite were used as standards for the following elements: Si, Ca, U, Ti, Fe, Pb, Al, Th, S, Na, K, V and P. Detection limits for these elements were ~0.01 wt.% (Table 1). U-Pb chemical ages of uranium mineral grains were calculated from the U, Th and Pb contents determined by electron microprobe data using the method described by Bowles (1990) and the equation by Cameron-Schiman (1978). The accuracy of Pb analyses by the electron microprobe is ~0.01%, which is equivalent to errors of 1 Ma for chemical ages. Our error estimations are in good agreement with the data reported by Bowles (1990).

4.2. Secondary ion mass spectrometry (SIMS) analysis

Polished thin sections from the MGJ uranium deposit were analyzed using a CAMECA 7f ion microprobe at the Department of

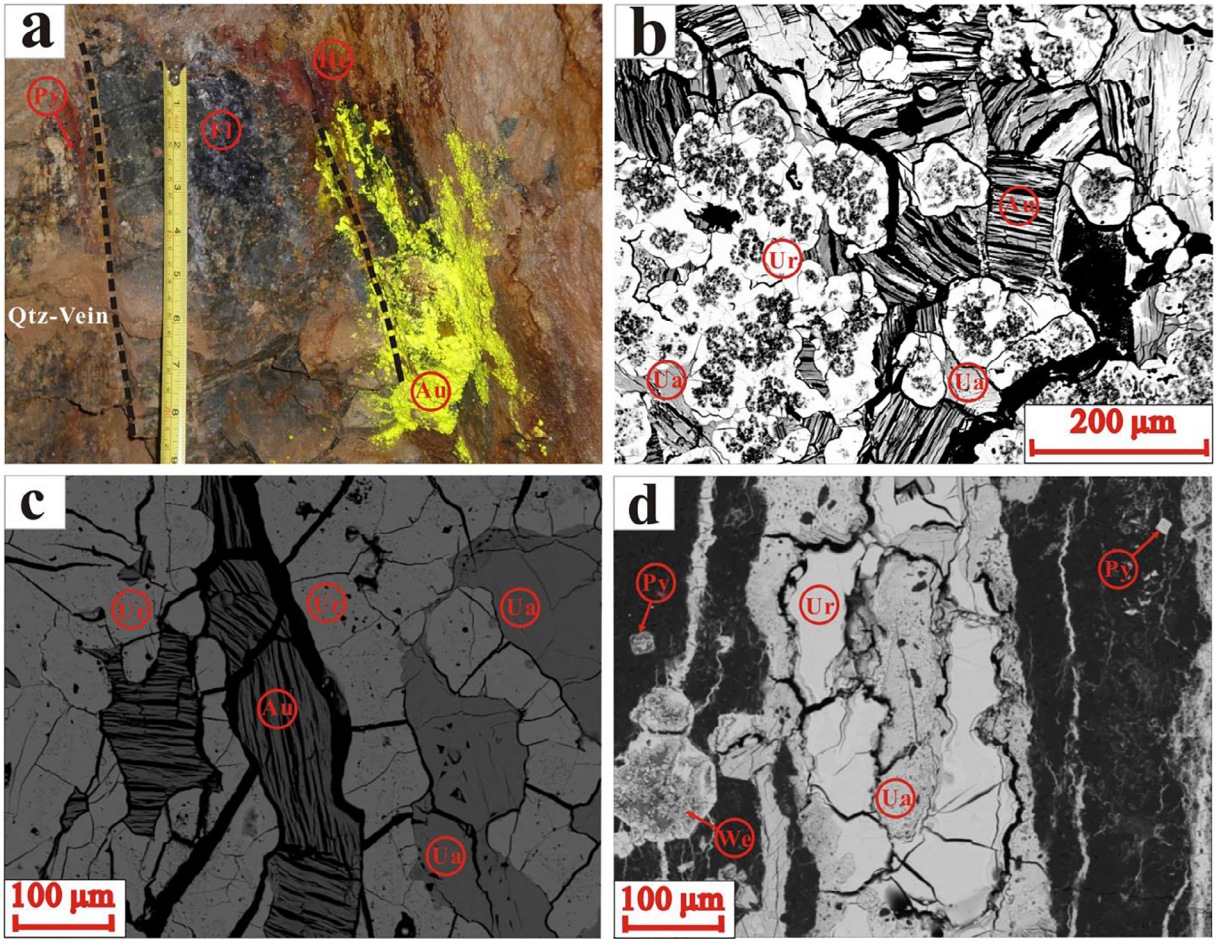

Fig. 3. (a) Image of outcrop showing uranium mineralization associated with quartz, fluotite and hematite. (b–d) BSE image of main uranium minerals at the MGJ deposit. Abbreviations: Qtz = Quartz. Py = Pyrite. Fl = Fluorite. He = Hematite. Ua = Uranophane. Ur = Uraninite. Au = Autunite. We = Weeksite.

Table 1
Oxide concentrations (wt.%) of uraninite from the MGJ deposit.

Comment	Na_2O	SiO_2	UO_2	CaO	Fe_2O_3	PbO	Al_2O_3	ThO_2	SO_2	K_2O	F	MgO	Cl	P_2O_5	TiO_2	V_2O_5	Total	Age (Ma)
MQ2N-7	0.12	0.21	86.02	2.19	0.56	0.04	0.15	0.00	0.15	0.00	0.18	0.00	0.00	0.76	0.10	0.00	90.48	2.21
MQ3N-10	0.13	0.11	84.88	2.39	0.43	0.02	0.13	0.02	0.12	0.11	0.13	0.00	0.00	1.05	0.06	0.00	89.59	2.23
MQ3N-16	0.12	0.69	87.18	2.12	0.55	0.02	0.44	0.00	0.20	0.06	0.12	0.00	0.02	0.99	0.07	0.00	92.55	2.29
MQ3N-19	0.10	0.44	85.54	2.30	0.45	0.02	0.32	0.00	0.17	0.07	0.06	0.00	0.02	1.28	0.10	0.00	90.86	2.29
MQ3N-21	0.10	0.14	86.25	2.34	0.39	0.03	0.21	0.00	0.13	0.06	0.22	0.00	0.01	1.24	0.06	0.02	91.21	2.25

Geological Sciences, University of Manitoba. Prior to analysis, the samples were cleaned with ethanol and polished with a 1 μm diamond-cleaning compound to remove the carbon coating. Then the cleaned polished sections were gold-coated to create a conductive surface on the sample. The samples selected for U–Pb geochronology contain the least-altered, most homogeneous uraninite grains.

The analytical protocol for U–Pb isotopic measurements is same as that used by Luo et al. (2015a). During analyses by SIMS, a mass-dependent bias (MDB) is commonly introduced to measurements. This bias is known as instrumental mass fractionation (IMF) and will typically favor the light isotope. Several processes contribute to IMF, the most influential of which are related to sample chemistry. Therefore, accurate isotopic analyses by SIMS require calibration using a mineral standard with a chemical composition similar to that of the mineral of interest. Lead isotopes measured by SIMS exhibit negligible instrumental fractionation during sputtering (Fayek et al., 2002a,b). We applied both medium mass resolution (DM/M 1300) and a voltage offset of –50 V, which minimized the mass interferences and matrix effects for uranium minerals with a range of Pb contents. Therefore, a natural crystal of pegmatite hosted uraninite (LAMNH) from the Scotty mine, Oxford County, Maine, was used to standardize the U–Pb isotopic analyses. The standard and minerals of interest were analyzed during the same analytical session.

The measured values of the LAMNH standard by SIMS during an analytical session was compared to the accepted isotopic composition, shown in Table 2 (Evins et al., 2001), to calculate a correction factor (α) using Eq. (1):

$$\alpha_{SIMS} = R_{SIMS}/R_{TIMS} \quad (1)$$

where R_{SIMS} is the isotopic ratio measured directly by SIMS and R_{TIMS} is the accepted or true ratio measured by thermal ionization mass spectrometry (TIMS) for standard. Where R = $^{206}Pb/^{238}U$, $^{207}Pb/^{235}U$, and $^{207}Pb/^{206}Pb$. The correction factor is then applied to the measurements of the unknown samples obtained during the same analytical session using Eq. (2) (Fayek et al., 2002b; Sharpe and Fayek, 2011):

$$R_{cor} = R_{SIMS}/\alpha \quad (2)$$

where R = $^{206}Pb/^{238}U$, $^{207}Pb/^{235}U$ and $^{207}Pb/^{206}Pb$. R_{cor} is the corrected isotopic ratio for the samples and RSIMS is the measured ratio for the samples.

The isotopic ratios ($^{206}Pb/^{238}U$ and $^{207}Pb/^{235}U$) were used to estimate ages for uraninite using ISOPLOT (Ludwig, 1993). U–Pb isotopic compositions of uraninites from the MGJ deposit and standard determined by SIMS are listed in Table 3.

5. Results

5.1. Chemical compositions of uraninite

The EMPA data for uraninite from the MGJ uranium deposit is listed in Table 1. Uranium minerals from the MGJ deposit show a limited compositional variation. The UO_2 contents vary from 84.88 to 87.18 wt.% with an average value of 85.97 wt.%. The CaO content ranges from 2.12 to 2.39 wt.% with an average value of 2.27 wt.%. In addition to UO_2 and CaO, the uraninite contains minor amounts of SiO_2 (0.11–0.44 wt.%) and P_2O_5 (0.76–1.28 wt.%) and trace PbO (0.02–0.04 wt.%), Na_2O (<0.13 wt.%), Fe_2O_3 (<0.56 wt.%), Al_2O_3 (<0.44 wt.%) and ThO_2 (<0.02 wt.%). The low totals observed can be explained by the presence of limited amount of water, undetected REEs, as well as the hexavalent uranium as the U was calculated as UO_2.

The uraninite grains in the deposit contain extremely low ThO_2, which is in agreement with their hydrothermal origin because Th has lower solubility in low to intermediate temperature (<300 °C) fluids (Cuney, 2010). Magmatic uraninite grains generally have CaO contents (up to 0.5 wt.%; Förster, 1999), much lower than low-temperature, hydrothermal uraninites with CaO up to 2.28 wt.% (Janeczek and Ewing, 1992). In the MGJ deposit, the uraninite grains contain high CaO contents (2.09–2.39 wt.%). Such high CaO contents cannot explained by contamination by some Ca-rich inclusions during the EMP analyses, as these grains are homogeneous under the BSE images and do not contain any inclusions of calcite or apatite. Therefore, the high CaO contents of the uraninite in the MGJ deposit are consistent with their hydrothermal origin. It is commonly considered that the incorporation of

Table 2
SIMS U-Pb data for uraninite from the MGJ uranium deposit corrected using LAMNH standard with Poisson% errors.

Sample	$^{206}Pb/^{204}Pb$	Possion%	$^{207}Pb/^{206}Pb$	Possion%	$^{235}U/^{238}U$	Possion%	$^{207}Pb/^{235}U$	Possion%	$^{206}Pb/^{238}U$	Possion%
MQ-4	3.06E+01	4.14E+01	1.43E−01	9.34E+00	7.55E−03	3.73E−01	1.85E−03	8.52E+00	9.48E−05	3.26E+00
MQ-6	4.93E+01	4.14E+01	1.06E−01	8.31E+00	7.57E−03	3.74E−01	2.22E−03	7.91E+00	1.58E−04	2.69E+00
MQ-8	6.00E+01	5.04E+01	1.10E−01	8.05E+00	7.52E−03	3.76E−01	2.60E−03	7.66E+00	1.79E−04	1.79E+00
MQ-9	2.57E+01	4.56E+01	1.27E−01	1.03E+01	7.49E−03	3.72E−01	1.47E−03	9.41E+00	8.86E−05	3.38E+00
LAMNH-1	1.12E+05	3.54E+01	5.45E−02	2.38E−01	7.62E−03	4.08E−01	3.06E−01	4.68E−01	4.28E−01	6.39E−02
LAMNH-2	9.87E+04	2.50E+01	5.39E−02	2.60E−01	7.60E−03	4.19E−01	2.81E−00	4.86E−01	3.95E−01	6.97E−02
LAMNH-3	7.33E+04	2.18E+01	5.40E−02	2.59E−01	7.61E−03	4.16E−01	2.61E−00	4.79E−01	3.67E−01	7.00E−02
LAMNH-4	8.48E+04	1.86E+01	5.43E−02	2.64E−01	7.57E−03	4.07E−01	2.59E−00	4.95E−01	3.61E−01	7.11E−02
Average	9.21E+04		5.42E−02		7.60E−03		2.77E+00		3.38E−01	
St. dev.	1.67E+04		2.68E−04		2.24E−05		2.22E−01		3.06E−02	
% Error(1σ)	0.18		0.00		0.00		0.08		0.08	
FF(a)	1.84E+00		1.01E−00		1.05E+00		6.73E−01		6.98E+00	

Table 3
Isotopic compositions of LAMNH standard measured by TIMS (Evins et al., 2001).

Standard	TIMS sample	$^{206}Pb/^{204}Pb$	$^{207}Pb/^{206}Pb$	$^{208}Pb/^{206}Pb$	$^{207}Pb/^{235}U$	$^{206}Pb/^{238}U$
LAMNH	MF-1a	4200	0.05388	0.00254	0.409	0.055
LAMNH	MF-3	>50,000	0.05377	0.00264	0.411	0.055
LAMNH	MF-3a	>50,000	0.05377	0.00264	0.411	0.056

Ca in the uraninite structure compensates for the charge difference due to the presence of U^{6+} (Janeczek and Ewing, 1992).

5.2. Chemical U-Pb age of uraninite

Chemical ages have previously been calculated to infer the formation ages of uraninite (e.g., Bowles, 1990; Cross et al., 2011). Based on the atomic percentage of Pb, U and Th, chemical ages could be calculated using Cameron-Schiman's equation given by Cameron-Schiman (1978):

$$t = Pb \times 10^{10}/(1.612U + 4.95Th) \quad (3)$$

which yields the age in years. In this study, the point determinations of uraninite grains cover a narrow interval of 2.2 to 2.3 Ma (Table 1), and the statistical processing shows that these uraninites are chronologically homogeneous with a weighted average of 2.3 ± 0.1 Ma (Fig. 4).

5.3. SIMS U–Pb age of uraninite

The SIMS U–Pb isotopic compositions of uraninites from the MGJ deposit are listed in Table 2. The results show that these uraninite grains have $^{235}U/^{207}Pb$ and $^{207}Pb/^{204}Pb$ varying from 385 to 680 and 3.26 to 6.60, respectively. We have calculated an SIMS U-Pb age of 1.9 ± 0.7 Ma using ISOPLOT (Ludwig, 1993) (Fig. 5), identical to the chemical age of 2.3 ± 0.1 Ma.

6. Discussion

6.1. Reliability of the uraninite U-Pb age

Although Bowles (1990) considered that many natural uraninites generally have low common Pb contents, this should not be assumed to be the case for all uraninites, such as the Xianshi

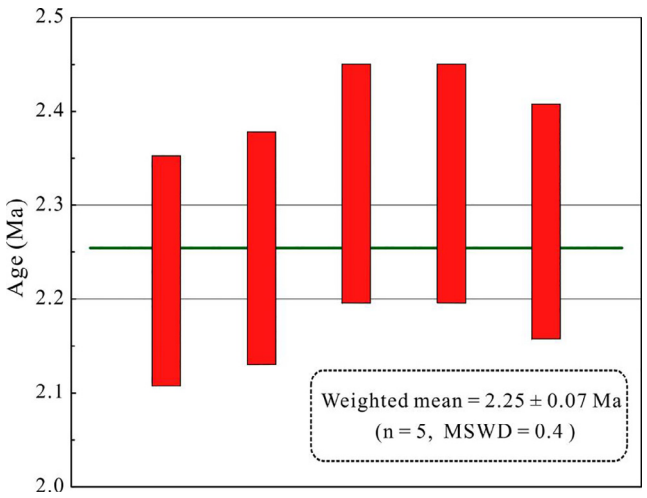

Fig. 4. Chemical Pb age (n = 5, 2σ error bars shown) and the weighted mean age for the MGJ uraninite using ISOPLOT (Ludwig, 1993).

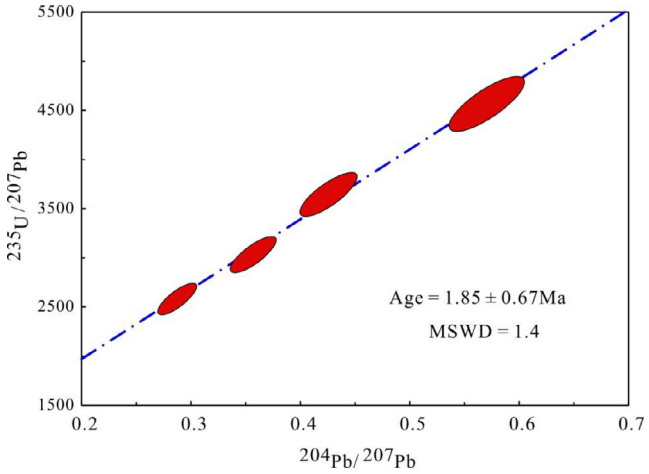

Fig. 5. SIMS uraninite U-Pb age from the MGJ uranium deposit.

uraninites with high common Pb from South China (Luo et al., 2015a). In this study, uraninites analyzed do not contain any measurable Th, and the range in uranium concentration is insufficient to estimate concentrations of initial common Pb using the isochron method of Suzuki and Adachi (1991). Therefore, our new EPMA chemical U–Th–Pb age is best interpreted as a reconnaissance-level age with control of determination the low common Pb content for the MGJ uraninite grains by SIMS U-Pb dating. This is the first data set to show that the SIMS U–Pb dating may be applicable for dating such young uraninite, 1.9 Ma. Additionally, such a young age is observed within a single polished thin section (Fig. 3).

This study suggests that the chemical U-Pb age (2.3 ± 0.1 Ma) for the MGJ deposit is undistinguishable from the precise ore-forming age of 1.9 ± 0.7 Ma obtained by SIMS. This similarity indicates that under specific circumstances (uraninite with low common Pb), chemical U-Pb ages can be reliable and used for dating uraninite (e.g., Bowles, 1990; Förster, 1999; Cross et al., 2011; Luo et al., 2015b). However, the limitations of the chemical U-Pb dating must also be noted because this chemical U-Th-Pb age is not required to determine the amount of common Pb.

Uranium mineralization in South China has occurred in more than one episode, as revealed by multiple stages of uranium-bearing veins (e.g., Luo et al., 2015a). Several U-Pb isotopic ages of primary uranium minerals from different stages of uranium-bearing veins have been previously reported (e.g., Xu et al., 1988; Xu and Zhang, 1988; Fang et al., 2007; Hu et al., 2008 and reference therein; Shi et al., 2010; Tian et al., 2010; Hu et al., 2013; Luo et al., 2015a,b). Hu et al. (2008) have summarized that the timing of the uranium mineralization ranges from Cretaceous to Tertiary (145–25 Ma) in South China (Fig. 6), although their host rocks range in age from Precambrian to Jurassic. They also indicated that the uranium mineralization can be divided into six stages: ~135 Ma, 120 to 115 Ma, 90 to 85 Ma, 75 to 65 Ma, 50 to 40 Ma, and ~25 Ma (Fig. 6). Our new dating results of the MGJ deposit demonstrate that the uranium mineralization in this deposit (~1.9 Ma) represents the youngest episode of mineralization for the granite-hosted uranium deposits in South China.

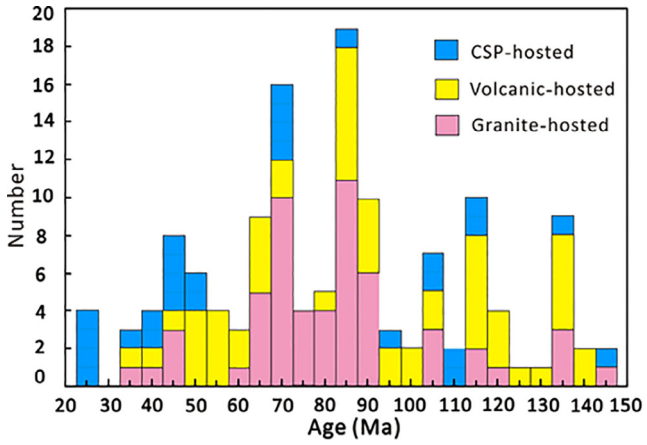

Fig. 6. Histogram showing the ages of uranium mineralization in South China. U-Pb ages of pitchblende (uraninite) from the three types of uranium deposits in South China, are mainly from Xu et al. (1988), Xu and Zhang (1988), Fang et al. (2007), Hu R.-Z. et al. (2008) and reference therein, Shi et al. (2010), Tian et al. (2010), Hu H. et al. (2013), Luo et al. (2015a,b). CSP = carbonaceous-siliceous-pelitic sedimentary rocks.

6.2. Implications for uranium metallogenesis

The major source of uranium for the MES uranium ore district is generally assumed to be the Douzhashan host granite (e.g., Min et al., 2003; Hu et al., 2012; Luo et al., 2015b; Zhao et al., 2016). Zhao et al. (2016) showed that the Douzhashan granite has extremely high uranium content up to 26 ppm, nine times higher than the average value of upper continental crust (2.7 ppm, Rudnick and Gao, 2003). Uranium occurs dominantly in tetravalent (U^{+4}) form in several types of minerals in granites, including uraninite (UO_2) and accessory minerals (e.g. monazite, thorite, zircon, apatite and xenotime). Indeed, abundant uraninite and uranium-bearing accessory minerals such as monazite, thorite, xenotime and zircon were identified in the Douzhashan two-mica granite (Hu et al., 2012; Zhao et al., 2016), whereas similar minerals are not observed in the Xiangcaoping biotite granite. Moreover, previous studies implied that uranium in uraninite and uranium-bearing accessory minerals can be easily leached by CO_2-rich fluids under the proper P, T, and Eh–pH conditions (McLennan and Taylor, 1979; Friedrich et al., 1987; Hu and Jin, 1990; Min et al., 1999; Skirrow et al., 2009; McGloin et al., 2015). In the MGJ deposit, such CO_2-rich fluids are well revealed by the fluid inclusion studies (Huang et al., 2012). We thus propose that the uranium-rich Douzhashan granites can be viable uranium source for the MGJ deposit. Such an interpretation is also supported by the fact that other large-scale uranium deposits (Shazijiang, Shuanghuajiang and Baimaochong) distributed in the Douzhashan granite (Fig. 2).

Previous studies proposed that crustal extension is closely associated with the intrusion of mafic dikes and the upward migration of mantle-derived CO_2 that mixed with CO_2-poor meteoric water (Jin and Hu, 1990; Hu et al., 1993, 2008, 2009; Chen et al., 2012). It was considered that the CO_2-rich fluids have leached uranium from pre-existing uranium-rich granites and have precipitated uranium-bearing minerals in faults and fractures to form the granite-hosted uranium deposits (e.g., Jin and Hu, 1990; Hu et al., 1993, 2008; Min et al., 1999, 2005; Chen et al., 2012; Luo et al., 2015a,b; McGloin et al., 2015). In the MGJ deposit, our new dating results indicate that the source of CO_2-rich, ore-forming fluids are likely sourced from the parent magmas of the synchronous Quaternary volcanic suite (2.1–1.2 Ma, Fan et al., 2006; Li et al., 2007). Fluids might have migrated along the NNE-trending fracture system that is synchronous with the spatially associated Quaternary volcanism (Fan et al., 2006; Fang et al., 2007; Li et al., 2007; Fig. 7). In addition, the active hot springs along the NNE-trending fracture system are also likely the potential source of CO_2-rich hydrothermal fluids (Wang et al., 2015). The ascending CO_2-rich fluids may leach uranium from granitic source rocks, and transport the uranium as soluble $UO_2(CO_3)_2^{2-}$ and $UO_2(CO_3)_3^{4-}$ complexes (Cuney, 1978; Leroy, 1978; McLennan and Taylor, 1979; Hu and Jin, 1990; Hu et al., 1993, 2008; Min et al., 1999). Precipitation of uranium minerals along NNE-trending fracture zones could have been triggered by a number of processes, including CO_2 degassing, decreasing P and T, changing Eh–pH conditions, and reduction of U^{6+} to U^{4+} by oxidation of Fe-bearing minerals such as biotite in the host granite, as evidenced by the close association of uranium-bearing minerals and hematite in the MGJ deposit (Fig. 3a).

This study provides a good example that uranium mineralization can be present at least 200 Ma later than the intrusion age of the hosting granites. Similar granite-hosted uranium deposits elsewhere in the world have also been suggested to be linked to

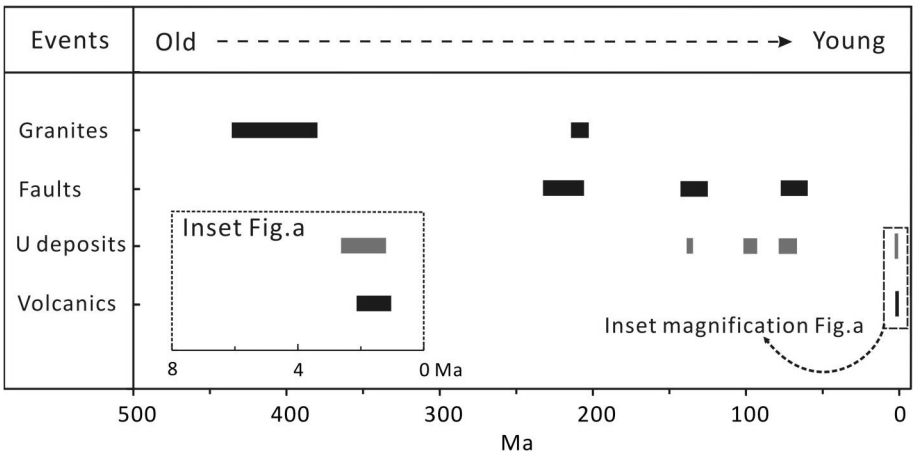

Fig. 7. The time sequence of the tectonic-magmatic-metallogenic events in the MES granitic complex. The inset magnification Fig. a shows ore-forming age from the MGJ deposit and eruption ages from Quaternary volcanics in South China. Zircon U-Pb age for these granites are from Zhao et al. (2013) and (2014). Formation ages of faults are from Fang et al. (2007). Ore-forming age of these uranium deposits in the MES uranium ore district are mainly based on the studies by Xu et al. (1988), Xu and Zhang (1988), Fang et al. (2007), Hu R-Z. et al. (2008), Shi et al. (2010), Hu H.et al. (2013), Luo et al. (2015b), and this study. Eruption ages for the Quaternary volcanics in South China are mainly based on the data from Li et al. (2007) and Fan et al. (2006).

the emplacement of mafic dikes or crustal extension, rather than the host granites. For example, uranium deposits that have uranium sourced from Hercynian granites of the La Crouzille district of the Massif Central, France were genetically related to the late intrusion of lamprophyre dykes and the associated crustal stretching event (e.g., Cuney, 1978; Leroy, 1978; Turpin et al., 1990). Therefore, our new findings that formation of the MGJ deposit is temporally related to crustal extension or the eruption of Quaternary volcanos (2.1–1.2 Ma, Fan et al., 2006; Li et al., 2007), providing the new implications for regional metallogeny. It is proposed that the MGJ deposit and other similar deposits in the region may have formed from a similar model including initial uranium leaching from host granites and later precipitation of uranium minerals along faults to form vein-type uranium mineralization. This study highlights that future exploration in this region should pay more attention to the uranium-rich granites, associated faults and Quaternary volcanic rocks.

7. Conclusions

This study report firstly a robust SIMS U-Pb age of 1.9 ± 0.7 Ma for the MGJ uranium deposit in the MES uranium ore district. The new, accurate SIMS U–Pb uraninite age is interpreted as a newly identified mineralization epoch in South China, making the MGJ deposit the youngest granite-hosted uranium deposit to the best of our knowledge. Therefore, the uranium mineralization in the deposit is likely genetically related to the Quaternary volcanic activities in the region. Further mineral exploration in this region will be benefited from these new findings.

Acknowledgements

This study was financially supported by Natural Science Foundation of China (41230316, 41603051), the National 973 Program of China (2014CB440906), the DREAM project of MOST China (2016YFC0600405) and the Strategic Priority Research Program (B) of CAS (XDB18030202), the CRC program and a NSERC Discovery Grant to Fayek, the CSC program to Luo. Special thanks to Ravinder Sidhu for her assistance with the EMPA and Ryan Sharpe for his help with the SIMS. The authors are grateful to the guest Editor Wei Terry Chen for dedicated editorial handling and two anonymous reviewers for their constructive comments and suggestions which helped us improve this paper.

References

Bowles, J.F.W., 1990. Age dating of individual grains of uraninite in rocks from electron microprobe analyses. Chem. Geol. 83 (1–2), 47–53.
Cameron-Schiman, M., 1978. Electron Microprobe Study of Uranium Minerals and Its Application to Some Canadian Deposit, University of Alberta, Edmonton. Thesis, pp. 1–343.
Chen, Y.W., Bi, X.W., Hu, R.Z., Dong, S.H., 2012. Element geochemistry, mineralogy, geochronology and zircon Hf isotope of the Luxi and Xiazhuang granites in Guangdong province, China. Implications for U mineralization. Lithos 150, 119–134.
Cross, A., Jaireth, S., Rapp, R., Armstrong, R., 2011. Reconnaissance-style EPMA chemical U-Th–Pb dating of uraninite. Aust. J. Earth Sci. 58, 675–683.
Cuney, M., 1978. Geologic environment, mineralogy, and fluid inclusions of the Bois Noirs-Limouzat urainum vein, Forez, France. Econ. Geol. 73, 1567–1610.
Cuney, M., 2010. Evolution of uranium fractionation processes through time: driving the secular variation of uranium deposit types. Econ. Geol. 105, 553–569.
Deng, P., Ren, J.S., Ling, H.F., Shen, W.Z., Sun, L.Q., Zhu, B., Tan, Z.Z., 2012. SHRIMP zircon U-Pb ages and tectonic implications for Indosinian granitoids of southern Zhuguangshan granitic composite, South China. Chin. Sci. Bull. 57, 1542–1552.
Dolníček, Z., René, M., Hermannová, S., Prochaska, W., 2014. Origin of the Okrouhlá Radouň episyenite-hosted uranium deposit, Bohemian Massif, Czech Republic: fluid inclusion and stable isotope constraints. Miner. Depos. 49, 409–425.
El-Naby, H.H.A., 2009. High and low temperature alteration of uranium and thorium minerals, Um Ara granites, south Eastern Desert, Egypt. Ore Geol. Rev. 35, 436–446.
Evins, L.Z., Sunde, T., Schöberg, H., Fayek, M., 2001. U and Pb isotope calibration of uraninite and galena standards for SIMS: SKB Technical Report 01-35, Svensk Kärnbränslehantering AB, pp. 1–48.
Fan, Q.C., Sun, Q., Long, A.M., Yin, K.J., Sui, J.L., Li, N., Wang, T.H., 2006. Geology and eruption story of volcanoes in Weizhou Island and Xieyang Island, Borthern Bay. Acta Petrol. Sin. 22, 1529–1537 (in Chinese with English abstract).
Fang, S.Y., Fan, L.T., Zhu, K.R., Shu, X.J., Ou-Yang, P.P., Xiao, J.J., 2007. Study on mineral ization structures of vein shape granite type uranium deposit and prospecting prognosis in Menggongjie. Uran. Geol. 23, 138–144 (in Chinese with English abstract).
Fayek, M., Harrison, M.T., Ewing, R.C., Grove, M., Coath, C.D., 2002a. O and Pb isotopic analyses of uranium minerals by ion microprobe and U-Pb ages from the Cigar Lake deposit. Chem. Geol. 185, 205–225.
Fayek, M., Kyser, T.K., Riciputi, L.R., 2002b. U and Pb isotope analysis of uranium minerals by ion microprobe and the geochronology of the McArthur River and Sue Zone uranium deposits, Saskatchewan, Canada. Can. Mineral. 40, 1553–1569.
Förster, H.J., 1999. The chemical composition of uraninite in Variscan granites of the Erzgebirge, Germany. Mineral. Mag. 63, 239–252.
Friedrich, M., Cuney, M., Poty, B., 1987. Uranium geochemistry in peraluminous leucogranites. Uranium 3, 353–385.
Helmy, H.M., Kaindl, R., Shibata, T., 2014. Genetically related Mo-Bi-Ag and U-F mineralization in A-type granite, Gabal Gattar, Eastern Desert, Egypt. Ore Geol. Rev. 62, 181–190.
Hu, R.Z., Jin, J.F., 1988. Genesis and origin of the guidong granitic batholith. J. Chengdu Coll. Geol. 15, 17–25 (in Chinese with English abstract).
Hu, R.Z., Jin, J.F., 1990. Mechanism of the migration and deposition of uranium in ascending hydrothermal solutions: evidence from the Xiwang uranium deposit. Geol. Rev. 36, 325–331 (in Chinese with English abstract).
Hu, R.Z., Li, C.Y., Ni, S.J., Liu, L., Yu, J.S., 1993. Research on ΣCO_2 source in ore-forming hydrothermal solution of granite type uranium deposits, South China. Sci. China Ser. D Earth Sci. 36, 1252–1262.
Hu, R.Z., Bi, X.W., Su, W.C., Peng, J.T., Li, C.Y., 2004. The relationship between uranium metallogenesis and crustal extension during the Cretaceous-Tertiary in South China. Earth Sci. Fornt. 11, 153–160 (in Chinese with English abstract).
Hu, R.Z., Bi, X.W., Zhuo, M.F., Peng, J.T., Su, W.C., Liu, S., Qi, H.W., 2008. Uranium metallogenesis in South China and its Relationship to crustal extension during the Cretaceous to Tertiary. Econ. Geol. 103, 583–598.
Hu, R.Z., Burnard, P.G., Bi, X.W., Zhuo, M.F., Peng, J.T., Su, W.C., Zhao, J.H., 2009. Mantle-derived gaseous components in ore-forming fluids of the Xiangshan uranium deposit, Jiangxi province, China. Evidence from He, Ar and C isotopes. Chem. Geol. 266, 86–95.
Hu, R.Z., Zhou, M.F., 2012. Multiple Mesozoic mineralization events in South China-an introduction to the thematic issue. Miner. Depos. 47 (6), 579–588.
Hu, H., Wang, R.C., Chen, W.F., Ding, H.H., Chen, P.R., Ling, H.F., 2012. Study on uranium source minerals of Douzhashan uranium-bearing granite, northeastern Guangxi. Geol. Rev. 58, 1056–1068 (in Chinese with English abstract).
Hu, H., Wang, R.C., Chen, W.F., Chen, P.R., Ling, H.F., Zhang, G.M., 2013. Timing of hydrothermal activity associated with the Douzhashan uranium-bearing granite and its significance for uranium mineralization in northeastern Guangxi, China. China Sci. Bull. 58, 4319–4328.
Huang, H.Y., Tan, Z.Y., Li, D.Y., 2012. Integrated prospecting model for uranium deposit in Menggongjie area of Hunan province. Uran. Geol. 28, 129–137 (in Chinese with English abstract).
Janeczek, J., Ewing, R., 1992. Dissolution and alteration of uraninite under reducing conditions. J. Nucl. Mater. 190, 157–173.
Jin, J.F., Hu, R.Z., 1990. Physicochemical conditions of mineralization of XW uranium deposit. J. Chengdu Coll. Geol. 17, 1–9 (in Chinese with English abstract).
Kribek, B., Zak, K., Spangenberg, J.E., Jehlicka, J., Prokes, S., Kominek, J., 1999. Bitumens in the late Variscan hydrothermal vein-type uranium deposit of Pribram, Czech Republic; sources, radiation-induced alteration, and relation to mineralization. Econ. Geol. 94, 1093–1114.
Li, Z.X., Li, X.H., 2007. Formation of the 1300-km-wide intracontinental orogen and postorogenic magmatic province in Mesozoic South China: a flat-slab subduction model. Geology 35 (2), 179–182.
Li, N., Fan, Q.C., Wang, T.H., Sun, Q., Sui, J.L., 2007. Preliminary study on K-Ar Chronology, petrology and geochemistry of Yandunling volcanic rocks, Hepu country, Guangxi. Acta Petrol. Sin. 23, 1423–1430 (in Chinese with English abstract).
Li, Z.Y., 2006. Hostspot uranium metallogenesis in South China. Uran. Geol. 22, 65–69 (in Chinese with English abstract).
Leroy, J., 1978. The Margnac and Fanay uranium deposits of the La Crouzille district (western Massif Central, France): geologic and fluid inclusion studies. Econ. Geol. 73, 1611–1634.
Ludwig, K.R., 1993, ISOPLOT: A plotting and regression program for radiogenic-isotope data: U.S. Geological Survey, Open File Report. 91-445, pp. 1–42.
Luo, J.C., Hu, R.Z., Fayek, M., Li, C.S., Bi, X.W., Abdu, Y., Chen, Y.W., 2015a. In-situ SIMS uraninite U-Pb dating and genesis of the Xianshi granite-hosted uranium deposit, South China. Ore Geol. Rev. 65, 968–978.
Luo, J.C., Hu, R.Z., Shi, S.H., 2015b. Timing of uranium mineralization and geological implications of Shazijiang granite-hosted uranium deposit in Guangxi, South China: new constraint from chemical U-Pb age. J. Earth Sci. 26 (6), 911–919.
McGloin, M.V., Tomkins, A.G., Webb, G.P., Spiers, K., MacRae, C.M., Paterson, D., Ryan, C.G., 2015. Release of uranium from highly radiogenic zircon through metamictization: the source of orogenic uranium ores. Geology 14, 15–18.

McLennan, S.M., Taylor, S.R., 1979. Rare earth element mobility associated with uranium mineralization. Nature 282, 247–249.
Min, M.Z., Luo, X.Z., Du, G.S., He, B.A., Campbell, A.R., 1999. Mineralogical and geochemical constraints on the genesis of the granite-hosted Huangao uranium deposit, SE China. Ore Geol. Rev. 14, 105–127.
Min, M.Z., Luo, X.Z., Li, X.G., Yang, Z., Zhai, L.Y., 2003. Geochemical constraints on the petrogenesis of the Middle Miaoershan granitoids, South China. Geochem. J. 37, 603–625.
Min, M.Z., Fang, C.Q., Fayek, M., 2005. Petrography and genetic history of coffinite and uraninite from the Liueryiqi granite-hosted uranium deposit, SE China. Ore Geol. Rev. 26, 187–197.
Rudnick, Gao, S., 2003. Composition of the continental crust. Treatise on Geochemistry, vol. 3. Elsevier, pp. 1–64 (Chapter 22).
Sharpe, R., Fayek, M., 2011. The world's oldest observed primary uraninite. Can. Mineral. 49, 1199–1210.
Shi, S.H., Hu, R.Z., Wen, H.J., Sun, R.L., Wang, J.S., Chen, H., 2010. Geochronology of the Shazijiang uranium ore deposit, northern Guangxi, China: U-Pb ages of pitchblende and their geological significance. Acta Geol. Sinica 84, 1175–1182 (in Chinese with English abstract).
Skirrow, R.G., Jaireth, S., Huston, D.L., Bastrakov, E.N., Schofield, A., van der Wielen, S.E., Barnicoat, A.C., 2009. Uranium mineral systems: processes, exploration criteria and a new deposit framework. Geosci. Aust. Rec. 20, 1–44.
Suzuki, K., Adachi, M., 1991. Precambrian provenance and Silurian metamorphism of the Tsubonosawa paragneiss in the South Kitakami Terrane, Northeast Japan, revealed by the chemical Th-U-Total Pb isochron ages of monazite, zircon and xenotime. Geochem. J. 25, 357–376.
Tian, J.J., Hu, R.Z., Su, W.C., Zhang, G.Q., Shang, P.Q., 2010. Ore U-Pb isochron ages and metallogenic tectonic setting of No. 661 uranium deposit. Min. Deposits 29 (3), 452–460 (in Chinese with English Abstract).
Turpin, L., Leroy, J.L., Sheppard, S.M.F., 1990. Isotopic systematics (O, H, C, Sr, Nd) of superimposed barren and U-bearing hydrothermal systems in a Hercynian granite, Massif Central, France. Chem. Geol. 88, 85–98.
Wang, L.X., Ma, C.Q., Lai, Z.X., Marks, M.A., Zhang, C., Zhong, Y.F., 2015. Early Jurassic mafic dykes from the Xiazhuang ore district (South China): implications for tectonic evolution and uranium metallogenesis. Lithos 239, 71–85.
Xu, W.C., Huang, S.J., Xia, Y.L., 1988. The study of U-Pb isotopic evolutionary system in chanziping uranium deposit. J. East China Coll. Geol. 11, 11–21 (in Chinese with English abstract).
Xu, W.C., Zhang, Y.H., 1988. The distribution pattern study of rare earth elements of pitchblende in three types of uranium deposits in northeast Guangxi Province. Uran. Geol. 4, 94–98 (in Chinese with English abstract).
Zhao, J.H., Zhou, M.F., Yan, D.P., Zheng, J.P., Li, J.W., 2011. Reappraisal of the ages of Neoproterozoic strata in South China: no connection with the Grenvillian orogeny. Geology 39, 299–302.
Zhao, K.D., Jiang, S.Y., Sun, T., Chen, W.F., Ling, H.F., Chen, P.R., 2013. Zircon U-Pb dating, trace element and Sr-Nd-Hf isotope geochemistry of Paleozoic granites in the Miao'ershan-Yuechengling batholith, South China: Implication for petrogenesis and tectonic-magmatic evolution. J. Asian Earth Sci. 74, 244–264.
Zhao, K.D., Jiang, S.Y., Ling, H.F., Palmer, M.R., 2014. Reliability of LA-ICP-MS U-Pb dating of zircons with high U concentrations: a case study from the U-bearing Douzhashan granite in South China. Chem. Geol. 389, 110–121.
Zhao, K.D., Jiang, S.Y., Ling, H.F., Sun, T., Chen, W.F., Chen, P.R., Pu, W., 2016. Late Triassic U-bearing and barren granites in the Miao'ershan batholith, South China: petrogenetic discrimination and exploration significance. Ore Geol. Rev. 77, 260–278.
Zhou, X.M., Sun, T., Shen, W.Z., Shu, L.S., Niu, Y.L., 2006. Petrogenesis of Mesozoic granitoids and volcanic rocks in South China: a response to tectonic evolution. Episodes 29 (1), 26–33.